

# Gas hydrate formation in the system $C_2H_6-H_2-H_2O$ at pressures up to 250 MPa

Sergey S. Skiba · Eduard G. Larionov ·  
Andrey Yu. Manakov · Sergey I. Kozhemjachenko

Received: 30 September 2009 / Accepted: 25 November 2009 / Published online: 10 December 2009  
© Springer Science+Business Media B.V. 2009

**Abstract** Decomposition curves of gas hydrates formed in the ethane–hydrogen–water system were studied in the pressure interval 2–250 MPa. Gas hydrates synthesized at low (up to 5 MPa) pressures were also studied with use of X-ray powder diffraction and Raman spectroscopy. It was shown that ethane–hydrogen mixtures with hydrogen contents 0–30 mol.% form cubic structure I gas hydrates. Higher hydrogen concentration most probably results in appearance of another hydrate phase. We speculate that the gas mixtures with the hydrogen content above 60 mol.% form cubic structure II double hydrate of hydrogen and ethane at temperatures below  $\approx 280$  K and pressures above 25 MPa.

**Keywords** Gas hydrate · Ethane · Hydrogen · Phase diagram · High pressure

## Introduction

Clathrate hydrates are crystalline inclusion compounds in which water molecules build polyhedral framework and guest molecules are included in the cavities of this framework [1]. Most of gas hydrates which exist at moderate pressures may be assigned to one of three structural types, namely cubic structure I (CS-I), cubic structure II

(CS-II) and hexagonal structure III (HS-III or sH) [1]. Detailed review of structures and properties of gas hydrates are presented in [1].

At present hydrogen is concerned to be prospective energy carrier, but economically sounded ways to store this gas has not been found yet. The idea to store hydrogen in a form of clathrate hydrate has been proposed recently [2–4]. It looks evident that gas hydrate technologies may be used in separation of gas mixtures containing hydrogen. Finally, hydrogen itself represents unusual guest species in gas hydrate chemistry because of small size of its molecule and extremely weak van-der-Waals interactions. Due to these reasons investigations of gas hydrates of pure hydrogen and gas hydrates containing hydrogen along with other guests are interesting and topical. Individual hydrogen hydrate contain up to 5 mass% of hydrogen [2] but it is stable at pressures above 100 MPa at temperatures close to 0 °C that embarrass storage of hydrogen in this form [5]. The authors of [6] propose to use a co-inclusion of additional guest species into the framework of hydrogen hydrate in order to stabilize it.

So far only limited data on mixed hydrate with hydrogen were available. Most of the mixed hydrates with cyclic organic liquids (like tetrahydrofuran or cyclohexanone) as a help-component were assigned to the CS-II hydrates. It was shown that in all cases the double hydrates are significantly more stable in comparison with the individual hydrogen hydrate, however the content of hydrogen in the double hydrates is considerably lower [6–9]. The same situation takes place in the case of formation of the CS-II double hydrate of propane and hydrogen [10]. Formation of the sH double hydrates with hydrogen was reported in [11]. The results concerning formation of gas hydrates in the ternary hydrogen–methane–water system have been published recently [12]. It was shown that gas mixtures with

S. S. Skiba · E. G. Larionov · A. Yu. Manakov (✉) ·  
S. I. Kozhemjachenko  
Nikolaev Institute of Inorganic Chemistry SB RAS, Ac.  
Lavrentiev ave. 3, 630090 Novosibirsk, Russian Federation  
e-mail: manakov@che.nsk.su

A. Yu. Manakov  
Novosibirsk State University, Pirogova Str. 2, 630090  
Novosibirsk, Russian Federation

hydrogen content up to 70 mol.% form CS-I methane hydrate; no co-inclusion of hydrogen were detected. In that case hydrogen plays a role of inert component which dilute methane in the gas phase and, as consequence, decrease its decomposition temperature [12]. The same results concerning co-inclusion of hydrogen into the framework of CS-I CO<sub>2</sub> hydrate were obtained in [13, 14] with use of Raman spectroscopy. Opposed results were obtained in [15] with use of NMR measurements. Some information concerning formation of double hydrates of hydrogen and tetraalkylammonium salts presented in [16–18].

Pure ethane forms with water a CS-I hydrate. Ethane molecules occupies 100% of the large cavities and only 5.8% of small cavities at ambient pressure [19]. Occupation of small cavities increases with the pressure rise [20]. Van-der-Waals diameter of ethane molecule ( $d_w = 5.5 \text{ \AA}$ , this value was calculated with use of the system of van-der-Waals radii presented in [21]) somewhat larger than the diameter of the small dodecahedral cavity (5.2 Å, [22]), hence inclusion of ethane molecule into this type of cavities results in unfavorable deformation of the hydrate framework. This situation is intermediate between methane hydrate (small cavities at least partially occupied by methane molecules, see e.g. [23]) and propane hydrate (no propane molecules are trapped in the small cavities) hence one can forecast more complicated picture of hydrate formation by ethane + hydrogen mixtures in comparison with hydrate formation by methane + hydrogen and propane + hydrogen mixtures. In this paper we present recent results concerning gas hydrate formation in the ethane–hydrogen–water system.

## Experimental

The samples of gas hydrates were synthesized from gas mixture and water in the experimental cell. In all the experiments we used distilled water and gases with a purity at least 99.9%. Gas mixtures were prepared by volumetric method with the error < 1 mol.%. Gas mixtures were loaded into the experimental cell with a slight excess (5–10 mol.%) with respect to water. Phase diagrams were investigated with use of differential thermal analysis (DTA) at high pressure. High-pressure equipment used in the work has been described in detail in [24]. Pressure was measured with Bourdon pressure gauge (measurement error 0.5%). Temperature was measured with a Chromel-Alumel (type K) thermocouple. Reproducibility of measured decomposition temperatures within one set of experiments was about 0.3 K. Approximating polynomials which fit the data set were chosen with use of a least squares procedure for each experimental curve (10–30 experimental points within the range 2–250 MPa).

Scattering of experimentally determined temperatures with respect to calculated values appeared to be close to Gaussian with a mean square deviation of a single measurement of about 0.7 K. We consider this value as the most correct estimation of the reliability of our results. It includes errors in measuring temperature, pressure, approximation error, and scatter of results between different sets of experiments. This value is somewhat larger than the scatter we obtained in case of gas hydrates formed by the single hydrate former. We explain this by the rather diffuse shape of the DTA signals and, consequently, high errors in determination of the position of this signal which are characteristic of gas hydrates with several components.

Hydrate samples for the powder diffraction investigation were prepared as follows. Finely crushed ice powder was placed into a high-pressure cell. Then hydrogen and ethane were supplied to the cell sequentially up to the total pressure 3–5 MPa. The sample was kept for 2–3 weeks at 269–272 K. The formation of the hydrate was monitored on the basis of pressure drop in the pressure vessel. Then the apparatus was cooled down to the liquid nitrogen temperature and the hydrate was extracted from it. The powder X-ray diffraction study was performed using synchrotron radiation at the 4-th beamline of the VEPP-3 storage ring (Siberian synchrotron and terahertz radiation center, Budker Institute of Nuclear Physics SB RAS), at  $\lambda = 0.3685 \text{ \AA}$ . The Debye–Scherrer scheme was applied. An MAR345 imaging plate detector (pixel dimension 100 μm) was used to record the powder diffraction pattern. The distance from the sample to the detector was calibrated using the diffraction patterns of a standard substance (NaCl). A fine-ground hydrate sample was placed in the cooled aluminum cell with two foam-coated holes for the primary beam and the outlet for diffracted radiation.

Raman spectra were recorded with a Triplemate SPEX spectrometer equipped with a multi-channel detector, LN-1340 PB, Princeton Instruments, in a back-scattering geometry. The spectral resolution was 1 cm<sup>-1</sup>. The 514.5 nm line of a 50 mW Ar ion laser was used for spectral excitation. Samples for Raman investigations were prepared in the same way as the samples for X-ray diffraction study. The only difference of the cell for Raman measurement is the sapphire window (working pressure up to 10 MPa) allowing *in situ* Raman measurement in the cell. All the spectra were recorded *in situ* at the temperature close to 273 K.

## Results and discussion

The experimental data are presented in Figs. 1, 2, 3. Positions of the experimental points in these figures correspond to the pressures and temperatures of endothermal

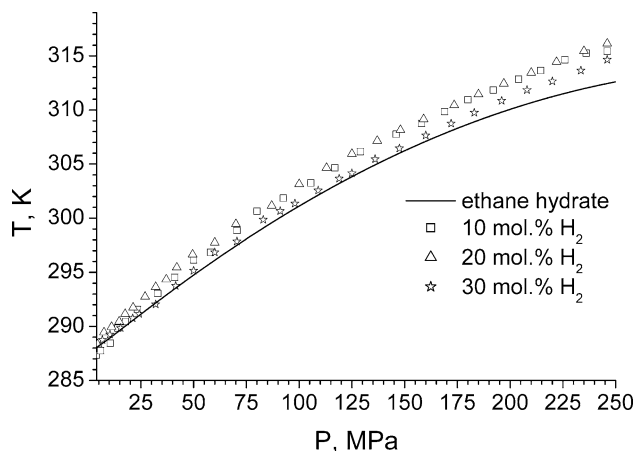


**Fig. 1** Decomposition curves of gas hydrates formed by pure ethane and ethane–hydrogen mixtures with 10, 20 and 30 mol.% of hydrogen

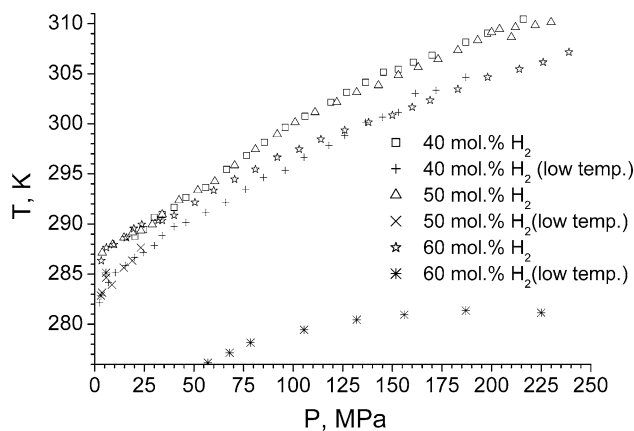


**Fig. 2** Decomposition curves and curves of monovariant equilibria of gas hydrates formed by ethane–hydrogen mixtures with 40, 50 and 60 mol.% of hydrogen. The monovariant curves are marked as “low temperature” curves

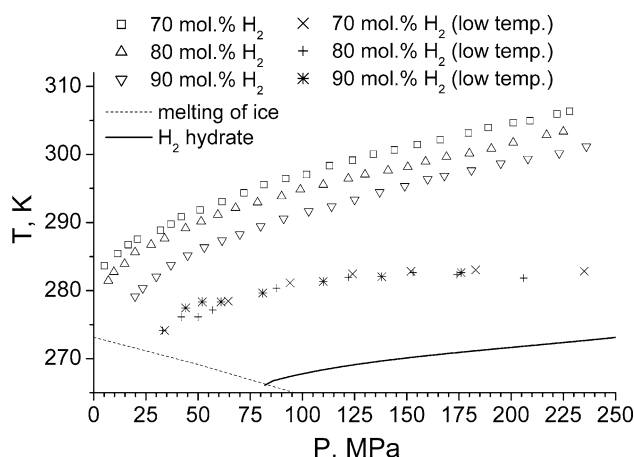


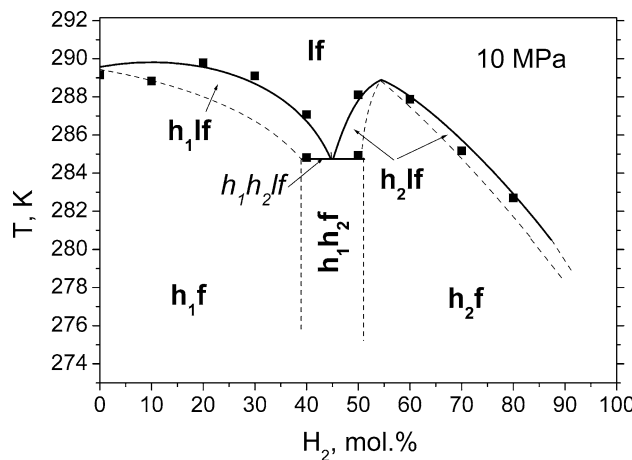
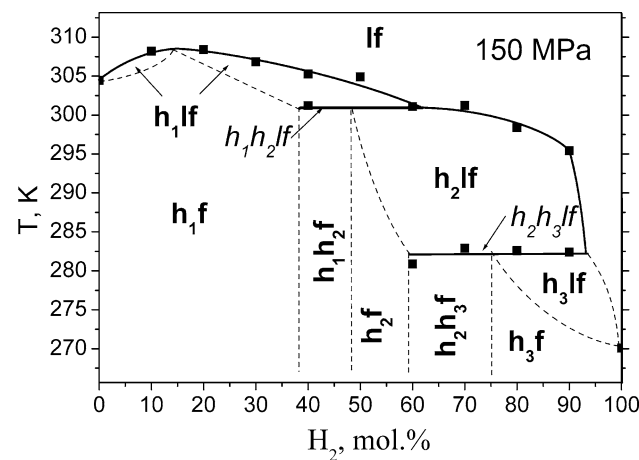
**Fig. 3** Decomposition curves and curves of monovariant equilibria of gas hydrates formed by ethane–hydrogen mixtures with 70, 80 and 90 mol.% of hydrogen. The monovariant curves are marked as “low temperature” curves

effects obtained in DTA experiments. Here and below we use following designations:  $h_1$ —the CS-I double ethane + hydrogen hydrate (solid solutions of hydrogen in the CS-I ethane hydrate);  $h_2$ —double ethane–hydrogen gas hydrate with unknown structure;  $h_3$ —the CS-II double ethane + hydrogen hydrate (solid solution of ethane in CS-II hydrogen hydrate);  $l$ —liquid phase;  $f$ —fluid phase. The coefficients of the equation approximating the experimental curves obtained at different compositions of the initial gas mixture are summarized in the Table 1. The isobaric sections of the system under investigation are shown in Figs. 4, 5. The points corresponding to the curves at corresponding pressures were re-calculated from the raw experimental data. The ethane–hydrogen mixture was considered as supercritical fluid for simplicity. The high temperature group of thermal effects corresponds to decomposition of gas hydrate into fluid and liquid phases. Here and below we refer these curves as liquidus curves. We speculate that two groups of low temperature effects (40–50 mol.%  $H_2$  and 60–90 mol.%  $H_2$ ) correspond to the monovariant equilibria realized in this system. The group of thermal effects denoted as  $h_1h_2lf$  most probably corresponds to monovariant decomposition curve of double ethane–hydrogen hydrate with unknown structure, we attribute the curve  $h_2h_3lf$  to decomposition of the CS-II double hydrate of hydrogen and ethane. We will discuss this point in more details in following sections.

Based on the specific features of the liquidus curves we divided our experimental curves into three groups characteristic of different intervals of concentrations: (1) 0–30 mol.% of hydrogen (Fig. 1), (2) 40–60 mol.% of hydrogen (Fig. 2) and (3) 60–90 mol.% of hydrogen in the initial gas mixture (Fig. 3). Let us discuss each of these groups in more details. In the interval of hydrogen concentrations corresponding to “group 1” the liquidus surface at low pressures is almost parallel to the concentration axis (Fig. 4). Pressure increase results in appearance of maximum at hydrogen concentration  $\sim 15$  mol.% (Fig. 5). We speculate that almost zero slope of the liquidus curve under the low-pressure conditions may be explained by the opposite influence of two factors: (1) decrease of the hydrate decomposition temperatures caused by dilution of ethane with hydrogen in the fluid phase and (2) increase of the hydrate stability due to co-inclusion of hydrogen into the small cavities. Increase of pressure results in increase of the occupancy of small cavities by ethane and hydrogen molecules. Appearance of the maximum on the liquidus curve under the high-pressure conditions shows that co-inclusion of ethane and hydrogen is more favorable in comparison with the pure ethane. We obtained X-ray powder patterns of the quenched sample of gas hydrates formed by gas mixtures with 23 mol.% of hydrogen (Table 2; Fig. 6). The samples was identified as the

**Table 1** The coefficients of equations  $T (\text{°C}) = A + B*P + C*P^2 + D*\ln P$  ( $P$ , MPa), that approximate the lines of liquidus and monovariant curves in the hydrogen–ethane–water system at pressures up to 250 MPa with the gas in excess

| $\text{C}_{\text{H}_2}$ (mol.%) | Pressure range (MPa) | A      | B       | C                       | D      |
|---------------------------------|----------------------|--------|---------|-------------------------|--------|
| Liquidus curves                 |                      |        |         |                         |        |
| 10                              | 2–246                | 12.20  | 0.1554  | $-2.079 \times 10^{-4}$ | 0.844  |
| 20                              | 2–246                | 13.73  | 0.1519  | $-1.926 \times 10^{-4}$ | 0.615  |
| 30                              | 2–246                | 14.07  | 0.1552  | $-1.955 \times 10^{-4}$ | 0.150  |
| 40                              | 20.3–232             | 12.07  | 0.1650  | $-2.307 \times 10^{-4}$ | 0.098  |
| 50                              | 25–230               | 6.70   | 0.1516  | $-2.449 \times 10^{-4}$ | 1.558  |
| 60                              | 2–239                | 12.79  | 0.1023  | $-9.734 \times 10^{-5}$ | 0.399  |
| 70                              | 5.1–228              | 7.09   | 0.1020  | $-1.269 \times 10^{-4}$ | 1.703  |
| 80                              | 7.0–225              | 1.41   | 0.0488  | $-7.209 \times 10^{-6}$ | 3.325  |
| 90                              | 19.8–236             | -13.27 | 0.0192  | $3.702 \times 10^{-5}$  | 6.350  |
| Monovariant curves              |                      |        |         |                         |        |
| 40                              | 2.5–187              | 7.63   | 0.0887  | $1.212 \times 10^{-5}$  | 1.367  |
| 50                              | 4–23                 | 9.52   | 0.2056  | 0                       | 0      |
| 60                              | 37–225               | -19.55 | 0.0182  | $-1.170 \times 10^{-4}$ | 5.426  |
| 70                              | 34–235               | -27.88 | -0.0180 | $-7.156 \times 10^{-5}$ | 8.371  |
| 80                              | 33–206               | -9.65  | 0.1186  | $-4.077 \times 10^{-4}$ | 2.089  |
| 90                              | 44–176               | 10.21  | 0.1629  | $-4.130 \times 10^{-4}$ | -3.213 |

**Fig. 4** Isobaric section of the phase diagram of ethane–hydrogen–water system at 10 MPa. Fluid phase was taken in excess.  $h_1$  CS-I double hydrate,  $h_2$  double hydrate with unknown structure,  $l$  liquid phase,  $f$  fluid phase. For more comments see the text**Fig. 5** Isobaric section of the phase diagram of ethane–hydrogen–water system at 150 MPa. Fluid phase was taken in excess.  $h_1$  CS-I double hydrate,  $h_2$  double hydrate with unknown structure,  $h_3$  CS-II double hydrate,  $l$  liquid phase,  $f$  fluid phase. For more comments see the text

mixtures of the CS-I gas hydrate and unreacted ice. In situ Raman spectra of the hydrate formed by the gas mixture with the same composition was recorded (Fig. 7). The band at  $991 \text{ cm}^{-1}$  corresponds to C–C vibrations of gaseous ethane, the other band at  $998 \text{ cm}^{-1}$  corresponds to C–C vibrations of ethane molecule trapped into large cavity of the CS-I framework [20]. We did not observe the bands corresponding to C–C vibrations of ethane molecule trapped into small cavity ( $\sim 1,022 \text{ cm}^{-1}$  [20]). Unfortunately,

we could not find reliable literature data concerning Raman spectra of  $\text{H}_2$  trapped in the cavities of CS-I framework. According to the data presented in [3, 6, 25, 26] the band corresponding to H–H vibrations of hydrogen molecule trapped into the small cavity of CS-II is situated near  $4,120 \text{ cm}^{-1}$  at the liquid nitrogen temperature. Taking into account general trends of the Raman bands temperature drift one should expect that at higher temperatures the bands will shift to higher wavenumber. Really, at the

temperatures close to 273 K the H–H vibration are situated at  $4,131\text{ cm}^{-1}$  [14] (CS-II propane +  $\text{H}_2$  hydrate) or  $4,136\text{ cm}^{-1}$  [16] (CS-II tetrahydrofuran +  $\text{H}_2$  hydrate). On the basis of these data we attribute the band at  $4,140\text{ cm}^{-1}$  to H–H vibrations of hydrogen molecule trapped into the small cavities of CS-I framework. Summarizing this section we can conclude that gas hydrates formed by the ethane–hydrogen mixtures with 0–30 mol.% of hydrogen correspond to the CS-I double hydrate of ethane and hydrogen or, equivalently, solid solutions of hydrogen in the CS-I ethane hydrate. We speculate that under the low-pressure conditions ethane molecules predominantly occupy the large cavities of this hydrate while the small cavities predominantly occupied by hydrogen molecules.

Decomposition curves of gas hydrates formed by the gas mixtures with 40 and 50 mol.% of hydrogen in the initial gas mixture are shown in Fig. 2. Two sets of thermal effects were obtained in both cases. The difference between “high temperature” and “low temperature” effects was about  $3\text{ }^{\circ}\text{C}$ . Appearance of the maximum of the liquidus

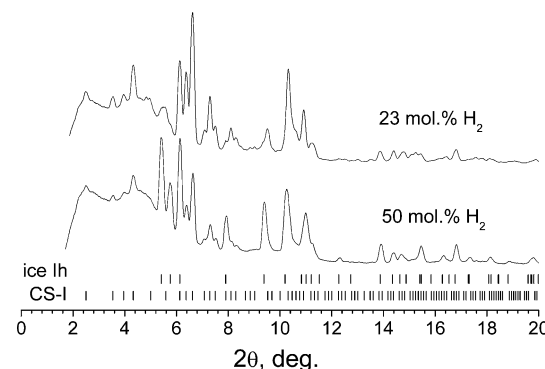


**Fig. 6** X-ray powder diffraction patterns of the quenched samples of gas hydrates, formed by the ethane–hydrogen system with different  $\text{H}_2$  contents in the initial gas mixture. More information presented in the Table 2

curve at about 55 mol.% of hydrogen (Fig. 4) and existence of the “low temperature” effects led us to the conclusion that, most probably, a new double ethane + hydrogen hydrate  $h_2$  appears in this interval of

**Table 2** Experimental and calculated values of  $2\theta$  for powder X-ray diffraction experiments

| Phase, hkl       | 23 mol.% $\text{H}_2$ , $-162\text{ }^{\circ}\text{C}$ CS-I,<br>$a = 11.92\text{ \AA}$ Ice Ih, $a = 4.50\text{ \AA}$ ,<br>$c = 7.32\text{ \AA}$ |  |       | 50 mol.% $\text{H}_2$ , $-165\text{ }^{\circ}\text{C}$ CS-I,<br>$a = 11.90\text{ \AA}$ Ice Ih, $a = 4.49\text{ \AA}$ ,<br>$c = 7.31\text{ \AA}$ |  |       | 80 mol.% $\text{H}_2$ , $-167\text{ }^{\circ}\text{C}$ CS-I,<br>$a = 11.94\text{ \AA}$ Ice Ih, $a = 4.50\text{ \AA}$ ,<br>$c = 7.34\text{ \AA}$ |  |       |
|------------------|---|--|-------|---|--|-------|---|--|-------|
|                  | $2\theta_{\text{obs}}$ ( $^{\circ}$ )   | $2\theta_{\text{calc}}$ ( $^{\circ}$ ) | I (%) | $2\theta_{\text{obs}}$ ( $^{\circ}$ )   | $2\theta_{\text{calc}}$ ( $^{\circ}$ ) | I (%) | $2\theta_{\text{obs}}$ ( $^{\circ}$ )   | $2\theta_{\text{calc}}$ ( $^{\circ}$ ) | I (%) |
| CS-I, (110)      | 2.503   | 2.499                                  | 7     | 2.496   | 2.503                                  | 9     | —   | —                                      | —     |
| CS-I, (200)      | 3.535   | 3.535                                  | 8     | 3.541   | 3.541                                  | 4     | 3.535   | 3.536                                  | 5     |
| CS-I, (210)      | 3.951   | 3.952                                  | 6     | 3.964   | 3.959                                  | 3     | 3.939   | 3.954                                  | 4     |
| CS-I, (211)      | 4.328   | 4.329                                  | 26    | 4.334   | 4.337                                  | 17    | 4.335   | 4.331                                  | 20    |
| ?                | 4.830   | —                                      | 4     | —   | —                                      | —     | 4.855   | —                                      | 12    |
| CS-I, (220)      | 4.980   | 4.999                                  | 7     | —   | —                                      | —     | 4.980   | 5.005                                  | 6     |
| Ice Ih, (100)    | 5.402   | 5.411                                  | 6     | 5.422   | 5.420                                  | 83    | 5.401   | 5.418                                  | 87    |
| CS-I, (310)      | 5.560   | 5.590                                  | 13    | 5.757   | 5.600                                  | 45    | 5.564   | 5.593                                  | 6     |
| Ice Ih, (002)    | 5.770   | 5.754                                  | 2     | —   | 5.763                                  | —     | 5.767   | 5.754                                  | 21    |
| CS-I, (222)      | 6.123   | 6.124                                  | 57    | 6.137   | 6.134                                  | 100   | 6.136   | 6.127                                  | 100   |
| Ice Ih, (101)    | 6.129   | —                                      | —     | 6.139   | —                                      | —     | —   | 6.135                                  | —     |
| CS-I, (320)      | 6.371   | 6.374                                  | 46    | 6.390   | 6.385                                  | 29    | 6.382   | 6.381                                  | 26    |
| CS-I, (321)      | 6.614   | 6.615                                  | 100   | 6.630   | 6.627                                  | 67    | 6.623   | 6.622                                  | 55    |
| CS-I, (400)      | 7.075   | 7.072                                  | 10    | 7.089   | 7.085                                  | 5     | —   | —                                      | —     |
| CS-I, (410)      | 7.291   | 7.290                                  | 38    | 7.305   | 7.303                                  | 23    | —   | —                                      | —     |
| CS-I, (411)(330) | 7.504   | 7.502                                  | 14    | 7.526   | 7.515                                  | 7     | —   | —                                      | —     |
| CS-I, (420)      | 7.912   | 7.902                                  | 5     | 7.922   | 7.914                                  | 36    | 7.903   | 7.905                                  | 29    |
| Ice Ih, (102)    | 7.908   | —                                      | —     | 7.922   | —                                      | —     | —   | 7.917                                  | —     |
| CS-I, (421)      | 8.094   | 8.104                                  | 13    | 8.133   | 8.118                                  | 7     | 8.099   | 8.113                                  | 12    |
| CS-I, (332)      | 8.297   | 8.295                                  | 11    | 8.328   | 8.309                                  | 5     | —   | —                                      | —     |
| ?                | 8.506   | —                                      | 2     | —   | —                                      | —     | —   | —                                      | —     |
| CS-I, (430)      | 8.852   | 8.844                                  | 1     | —   | —                                      | —     | —   | —                                      | —     |
| CS-I, (431)(510) | 9.016   | 9.0190                                 | 1     | —   | —                                      | —     | 9.029   | 9.019                                  | 3     |
| Ice Ih, (110)    | 9.355   | 9.378                                  | 5     | 9.405   | 9.394                                  | 58    | 9.398   | 9.385                                  | 69    |
| CS-I, (432)(520) | 9.499   | 9.526                                  | 23    | —   | —                                      | —     | 9.538   | 9.537                                  | 5     |

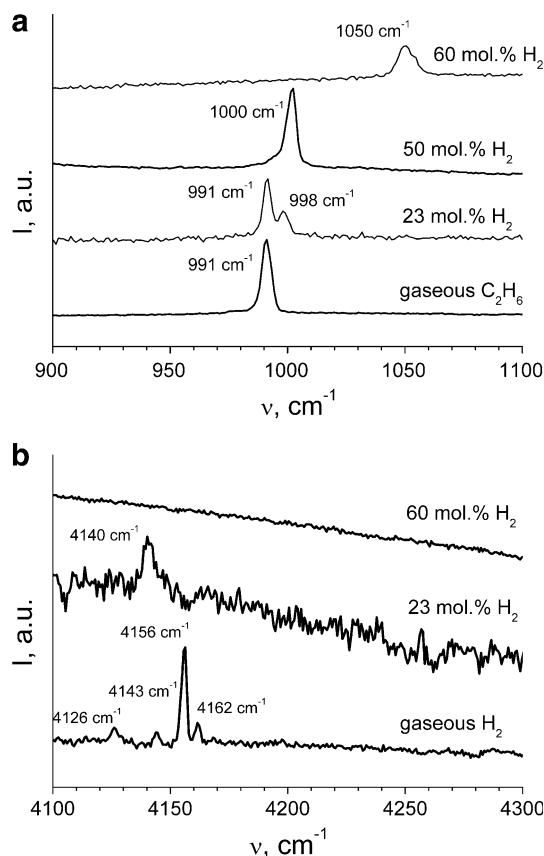


**Fig. 7** Raman spectra of pure gases and gas hydrates formed by the ethane–hydrogen system with different H<sub>2</sub> contents in the initial gas mixture. **a** C–C vibrations of the ethane molecule, **b** H–H vibrations of H<sub>2</sub> molecule

concentrations. We speculate that the “low temperature” effects correspond to the monovariant line  $h_1h_2lf$ . X-ray powder diffraction patterns of quenched samples of hydrates formed by the gas mixtures with 50 and 80 mol.% of hydrogen corresponded to CS-I (Fig. 6; Table 2). It is not clear whether the hydrates really belong to this structural type or CS-I hydrates were formed in the course of decomposition of gas hydrate with unknown structure caused by e.g. escape of hydrogen from the hydrate framework. Additional work is necessary to clarify this point. The Raman spectra of the hydrates formed by the gas mixture with the hydrogen content 50 and 60 mol.% are shown in Fig. 7. No bands corresponding to H–H vibrations were found. In the case of the sample formed by the gas mixture with 50 mol.% hydrogen content the position of the band corresponded to C–C vibration of the ethane molecule slightly differ from the spectrum of the CS-I ethane + hydrogen hydrate. Both these features of the Raman spectra well corresponded to reported in [14]. In addition, in some cases we obtained the spectra with the positions of C–C bands significantly different from the expected (Fig. 7). At present we cannot interpret these

spectra on the basis of available literature data. One of the probable explanations of these observations is joint inclusion of both ethane molecules and hydrogen molecules to the cavities of hydrate framework that may result in significant widening and shifts of the Raman bands. Concluding this section we should state that phase diagram gives evidence of formation of the new gas hydrate phase  $h_2$  but we can not perform the experiments which are necessary to prove the existence of this phase with use of X-ray and Raman spectroscopy methods (in situ X-ray diffraction etc.).

The DTA curves obtained with use of gas mixtures with 60–90 mol.% of hydrogen also contained two thermal effects. In this case “low temperature” effects occurred in the pressure interval 35–250 MPa. The difference in temperature between “high temperature” and “low temperature” effects was 17 °C at 50 MPa and 24 °C at 240 MPa (Figs. 2, 3). Pressure interval in which the “low temperature” effects occur roughly corresponds to the pressure interval in which CS-II hydrate of pure hydrogen exists (Fig. 3) [5]. In addition the curve formed by the “low temperature” effects has the dome-like shape what is characteristic of the hydrogen hydrate. We believe that the “low temperature” curve corresponds to monovariant line  $h_2h_3lf$  complied with decomposition of the CS-II double hydrate of hydrogen and ethane which represent itself solid solution of ethane in CS-II hydrogen hydrate. The data presented show that inclusion of ethane increases decomposition temperature of the double hydrate.

## Conclusion

On the basis of the obtained experimental results we conclude that three types of hydrates exist in the hydrogen–ethane–water system: CS-I double hydrate ethane and hydrogen ( $h_1$ ), double hydrate of ethane and hydrogen with unknown structure ( $h_2$ ) and CS-II double hydrate of hydrogen and ethane ( $h_3$ ).

**Acknowledgments** We thank Russian Foundation for Basic Research grant 08-03-00191-a for financial support of this work.

## References

1. Sloan, E.D.: Clathrate Hydrates of Natural Gases, 2nd edn. Marcel Dekker, New York (1998)
2. Struzhkin, V.V., Militzer, B., Mao, W.L., Mao, H.-k., Hemley, R.J.: Hydrogen storage in molecular clathrates. Chem. Rev. **107**, 4133–4151 (2007)
3. Mao, W.L., Mao, H.-k., Goncharov, A.F., Struzhkin, V.V., Guo, Q., Hu, J., Shu, J., Hemley, R.J., Somayazulu, M., Zhao, Yu.: Hydrogen clusters in clathrate hydrate. Science. **297**, 2247–2249 (2002)

4. Lokshin, K.A., Zhao, Yu., He, D., Mao, W.L., Mao, H.-k., Hemley, R.J., Lobanov, M.V., Greenblatt, M.: Structure and dynamics of hydrogen molecules in the novel clathrate hydrate by high pressure neutron diffraction. *Phys. Rev. Lett.*, **93**, contr. 125503 (2004)
5. Dyadin, Yu.A., Larionov, E.G., Manakov, A.Yu., Zhurko, F.V., Aladko, E.Ya., Mikina, T.V., Komarov, V.Yu.: Clathrate hydrates of hydrogen and neon. *Mendeleev. Commun.* 209–210 (1999)
6. Florusse, L.J., Peters, C.J., Schoonman, J., Hester, K.C., Koh, C.A., Dec, S.F., Marsh, K.N., Sloan, E.D.: Stable low-pressure hydrogen clusters stored in a binary clathrate hydrate. *Science*, **306**, 469–471 (2004)
7. Hester, K.C., Strobel, T.A., Sloan, E.D., Koh, C.A., Hug, A., Schultz, A.J.: Molecular hydrogen occupancy in binary  $H_2$ -THF clathrate hydrates by high resolution neutron diffraction. *J. Phys. Chem. B*, **110**, 14024–14027 (2006)
8. Anderson, R., Chapoy, A., Tohidi, B.: Phase relations and binary clathrate hydrate formation in the system  $H_2$ -THF- $H_2O$ . *Langmuir*, **23**, 3440–3444 (2007)
9. Lee, H., Lee, J.W., Kim, D.Y., Park, J., Seo, Y.T., Zeng, H., Moudrakovski, I.L., Ratcliff, C.I., Ripmeester, J.A.: Tuning clathrate hydrates for hydrogen storage. *Nature*, **434**, 743–746 (2005)
10. Skiba, S.S., Larionov, E.G., Manakov, A.Yu., Kolesov, B.A., Anchakov, A.I., Aladko, E.Ya.: Double clathrate hydrate of propane and hydrogen. *J. Incl. Phenom.*, **63**, 383–386 (2009)
11. Strobel, T.A., Koh, C.A., Sloan, E.D.: Water cavities of sH clathrate hydrate stabilized by molecular hydrogen. *J. Phys. Chem. B*, **112**, 1885–1887 (2008)
12. Skiba, S.S., Larionov, E.G., Manakov, A.Y., Kolesov, B.A., Kosyakov, V.I.: Investigation of hydrate formation in the system  $H_2$ - $CH_4$ - $H_2O$  at a pressure up to 250 MPa. *J. Phys. Chem. B*, **111**, 11214–11220 (2007)
13. Sugahara, T., Murayama, S., Hashimoto, S., Ohgaki, K.: Phase equilibria for  $H_2+CO_2+H_2O$  system containing gas hydrates. *Fluid Phase Equilib.*, **233**, 190–193 (2005)
14. Sugahara, T., Hashimoto, S., Mori, H., Sakamoto, J., Ogata, K., Ohgaki, K.: Cage occupancies of hydrogen molecule and thermodynamic stabilities of hydrogen-containing hydrates. In: Proceedings of the 6-th International Conference on Gas Hydrates (ICGH 2008), Vancouver, Canada, July 6–10 (2008)
15. Kim, D.-Y., Lee, H.: Spectroscopic identification of the mixed hydrogen and carbon dioxide clathrate hydrate. *J. Am. Chem. Soc.*, **127**, 9996–9997 (2005)
16. Hashimoto, S., Murayama, S., Sugahara, T., Ohgaki, K.: Thermodynamic and Raman spectroscopic studies on  $H_2 +$  tetrahydrofuran + water and  $H_2 +$  tetra-n-butyl ammonium bromide + water mixtures containing gas hydrates. *Chem. Eng. Sci.*, **61**, 7884–7888 (2006)
17. Chapoy, A., Anderson, R., Tohidi, B.: Low-pressure molecular hydrogen storage in semi-clathrate hydrates of quaternary ammonium compounds. *J. Am. Chem. Soc.*, **129**, 746–747 (2007)
18. Strobel, T.A., Koh, C.A., Sloan, E.D.: Hydrogen storage properties of clathrate hydrate materials. *Fluid Phase Equilib.*, **261**, 382–389 (2007)
19. Udachin, K.A., Ratcliff, C.I., Ripmeester, J.A.: Single crystal diffraction studies of structure I, II and H hydrates: structure, cage occupancy and composition. *J. Supramol. Chem.*, **2**, 405–408 (2002)
20. Morita, K., Nakano, S., Ohgaki, K.: Structure and stability of ethane hydrate crystal. *Fluid Phase Equilib.*, **169**, 167–175 (2000)
21. Zefirov, Y.V., Zorkii, P.M.: van-der-Waals radii and their application in chemistry. *Uspekhi Khimii*, **58**, 713–746 (1989)
22. Dyadin, Yu.A., Udachin, K.A.: Clathrate polyhydrates of peralkylonium salts and their analogs. *Russ. J. Struct. Chem.*, **28**, 394–432 (1987)
23. Klapproth, A., Goreshnik, E., Staykova, D., Klein, H., Kuhs, W.F.: Structural studies of gas hydrates. *Can. J. Phys.*, **81**, 503–518 (2003)
24. Dyadin, Y.A., Larionov, E.G., Mirinskij, D.S., Mikina, T.V., Aladko, E.Y., Starostina, L.I.: Phase diagram of the  $Xe-H_2O$  system up to 15 kbar. *J. Incl. Phenom.*, **28**, 271–285 (1997)
25. Kumar, R., Englezos, P., Moudrakovski, I., Ripmeester, J.A.: Structure and composition of  $CO_2/H_2$  and  $CO_2/H_2/C_3H_8$  hydrate in relation to simultaneous  $CO_2$  capture and  $H_2$  production. *AIChE J.*, **55**, 1584–1594 (2009)
26. Strobel, T.A., Sloan, E.D., Koh, C.A.: Raman spectroscopic studies of hydrogen clathrate hydrates. *J. Chem. Phys.*, **130**, contr. 014506 (2009)